Morphology control and optical properties of Bi_2O_3 crystals prepared by low-temperature liquid phase method

Jin Li ✉, *Ben Ze Wu, Zhen Xiang Zhou*

College of Physical Science and Technology, Xinjiang University, Urumqi 830046, People's Republic of China
✉ *E-mail: xjlijin@163.com*

Published in Micro & Nano Letters; Received on 11th January 2018; Revised on 17th May 2018; Accepted on 21st June 2018

γ-Bi_2O_3 powders were prepared from [$Bi(NO_3)_3{\cdot}5H_2O$] and NaOH through low-temperature liquid phase method at <90°C. This process featured low cost, simplicity and a normal pressure. Bismuth oxides were synthesised in large quantities in water systems. Morphology, structure and optical properties were characterised by X-ray diffraction, scanning electron microscopy (SEM), Fourier transform infrared spectroscopy (FTIR) and ultraviolet visible absorption spectrophotometry (UV–Vis). The SEM indicated that tetrahedral Bi_2O_3 with the edge length of 1–5 μm was formed. The FTIR spectra show a chemical bond of Bi–O existed. Bi_2O_3 presents the photo absorption properties from UV light region to visible light and the band gap of the Bi_2O_3 is 3.0 eV.

1. Introduction: Bismuth oxide (Bi_2O_3) is one of p-type semiconductor materials that have many excellent physical properties. Bi_2O_3 can be used as sensors [1–4], solid electrolyte in solid fuel cells [1–3] and photocatalysts [5–7]. Owing to its unique chemical and physical properties such as high-energy band gap, high refractive index, high dielectric permittivity, and excellent photoconductivity, Bi_2O_3 has been the focus of scientific research [8–10].

Several methods including sol–gel, flame spray pyrolysis, microemulsion, hydrothermal, metal organic chemical vapour deposition process, vapour phase deposition technique, electrospinning technique, microwave-assisted heating method have been successfully used for the fabrication of Bi_2O_3 with different morphology. Bi_2O_3 needles have been prepared using $Bi(NO_3)_3$ as the precursor and NaOH as a precipitating agent under a required thermal treatment of 450°C for 4 h by Irmawati *et al*. [11]. Cheng *et al*. [12] have reported a low-temperature synthesising α-phase Bi_2O_3 at 60°C and the products exhibit a flower-like architecture structure assembled by Bi_2O_3 micro-rods. Rod-like α-Bi_2O_3 and tetrahedral γ-Bi_2O_3 particles have been controlled fabricated by a facile solution crystallisation method [13]. Using different surfactants such as oleic acid [4], dodecylbenzenesulfonate [14], sodium ethylene glycol [15], and polyethylene glycol [16], other researchers have controlled the morphologies of Bi_2O_3 crystals with needle-like, flower-like or tetrahedral morphologies successfully. The researchers have discussed the important effect of above surfactants on the morphology of Bi_2O_3 products in detail. As far as we know, there are no reports about controlling the morphology of Bi_2O_3 products by heating ways.

This Letter aims to investigate the effect of Bi_2O_3 morphology through different ways of heating by a low-temperature liquid phase method. The Bi_2O_3 powders attained at 90°C possess a perfect tetrahedral and platelet shapes with a band gap of 3.0 eV. With their novel morphology and high-energy band gap, Bi_2O_3 powders have the potential to be applied to ultraviolet-visible-light-driven photocatalyst for environmental clean up and optoelectric devices for solar energy conversion to electricity.

2. Experiments

2.1. Experiments materials: Bismuth nitrate ($Bi(NO_3)_3{\cdot}5H_2O$), sodium hydroxide (NaOH, analytic grade) and nitric acid (HNO_3) were purchased from Aladdin Regent from Shanghai of China, Tianjin DaMao regent chemical company and Sichuan Xilong regent chemical company, respectively. All chemicals were of analytical grade and used without further purifications. Deionised water was used throughout the experiments.

2.2. Bismuth oxide preparation: To synthesise Bi_2O_3 crystals, 4.85 g $Bi(NO_3)_3{\cdot}5H_2O$ was first dissolved in mixed solvent of distilled water and nitric acid (HNO_3) under constant magnetic stirring at 70°C. To restrain hydrolysation of Bi^{3+}, the concentration of HNO_3 was kept 1 mol/L. Continuity adding NaOH into solution until did not produce the precipitate. The mixture was washed and filtered by deionised water for several times. After that the mixture was added to deionised water and adjusted pH by NaOH. Then as-prepared precursor was reflux condensation for 6 h. After that, the solid products were centrifuged, washed with distilled water and ethanol for several times to remove the ions possibly remaining in the final products, and finally dried at 80°C in a vacuum drier for 3 h. The bismuth-oxidation reaction can be presented as

$$Bi^{3+} + OH^- \rightarrow Bi(OH)_3 \quad (1)$$

$$Bi(OH)_3 + OH^- \rightarrow Bi(OH)_3^{3-x} \quad (2)$$

$$Bi(OH)_3^{3-x} \rightarrow Bi_2O_3 \quad (3)$$

The first procedure (1) was called precursor created, (2) was called precursor hydrolysed, (3) was called precursor polycondensation. According to (1)–(3), we can get the pure Bi_2O_3 power after a drying process.

2.3. Characterisations: The crystalline phase of products was identified by powder X-ray diffraction (XRD) using a Bruker D8 advanced X-ray diffractometer made in Germany with Cu Kα radiation ($\lambda = 1.54056$ Å) at 40 kV and 40 mA, and the 2θ range was from 10° to 80° with a speed of 5°/min. The images of scanning electron microscopy (SEM) were obtained using a Germany LEO 1430VP scanning electron microscope. The infrared spectrum was recorded on a Shimadzu IR spectrophotometer. The absorption spectrum was determined with an UV–Vis spectrophotometer (UV-Vis, Solid Spec-3700, Shimadzu, Japan).

3. Results and discussion

3.1. XRD analysis of as-prepared Bi_2O_3: The crystallinity and phase of Bi_2O_3 powders were checked by XRD patterns shown in Fig. 1. The broadening of peaks indicates its small crystallite size. All of the recorded diffraction peaks can be indexed to the

pure bcc space group with a cell parameter of $a = 10.08$ Å (JCPDS Card No. 74–1375), which confirm that the as-prepared products are pure γ-Bi_2O_3 phase. The strong and sharp peaks indicate that the products are highly crystallised. The pH value, molar ratio of $Bi(NO_3)_3{\cdot}5H_2O$ to NaOH, hydrothermal time and temperature are key factors in the formation of Bi_2O_3. In Fig. 1, the black line shows the calculated XRD pattern of γ-Bi_2O_3, and the blue and red ones were characterised at a lower temperature of 90°C with a pH value of 8 and 12 for 6 h. So we can draw conclusion that the pure γ-Bi_2O_3 can be formed in a basicity situation.

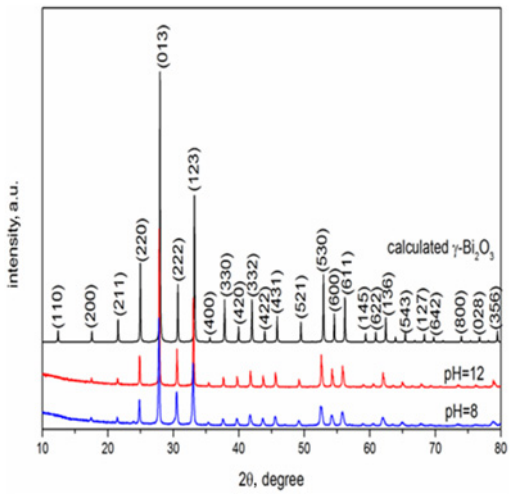

Fig. 1 *XRD pattern of as-prepared γ-Bi_2O_3 powder*

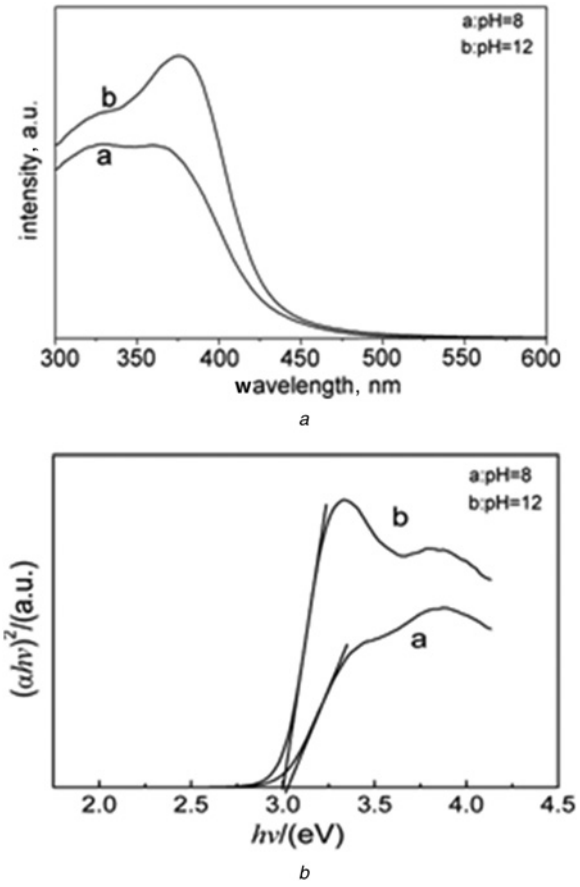

Fig. 2 *Optical absorption properties of Bi_2O_3 samples*
a UV–Vis absorption spectra of Bi_2O_3 samples
b Calculated band gap of Bi_2O_3 samples with the tangent of the linear part

Wu Yu-Chun *et al*. have discussed the formation of Bi_2O_3 in detail [17]. They have pointed out that the amount of HNO_3 and the adjustment of pH value by NaOH are most important factors during the formation of Bi_2O_3. In our experiment, during NaOH titration process, the pH value is almost no change but then sharply increased from 1 to 8 or to 12 when a specific amount of NaOH is added, the abrupt change of pH value was accompanied by the appearance of a precipitate with yellow-orange in colour. As shown in Fig. 2*a* following, Bi_2O_3 exhibits a strong light absorption at 400–450 nm corresponding to yellow-orange. So the colour of the solution transformation from white to yellow-orange can be regarded as the formation of Bi_2O_3. So pH value was considered as a key factor in this Letter.

3.2. Morphology of Bi_2O_3 powder

3.2.1. Tetrahedron: The morphologies of the products were demonstrated by SEM images displayed in Fig. 3. Well-defined

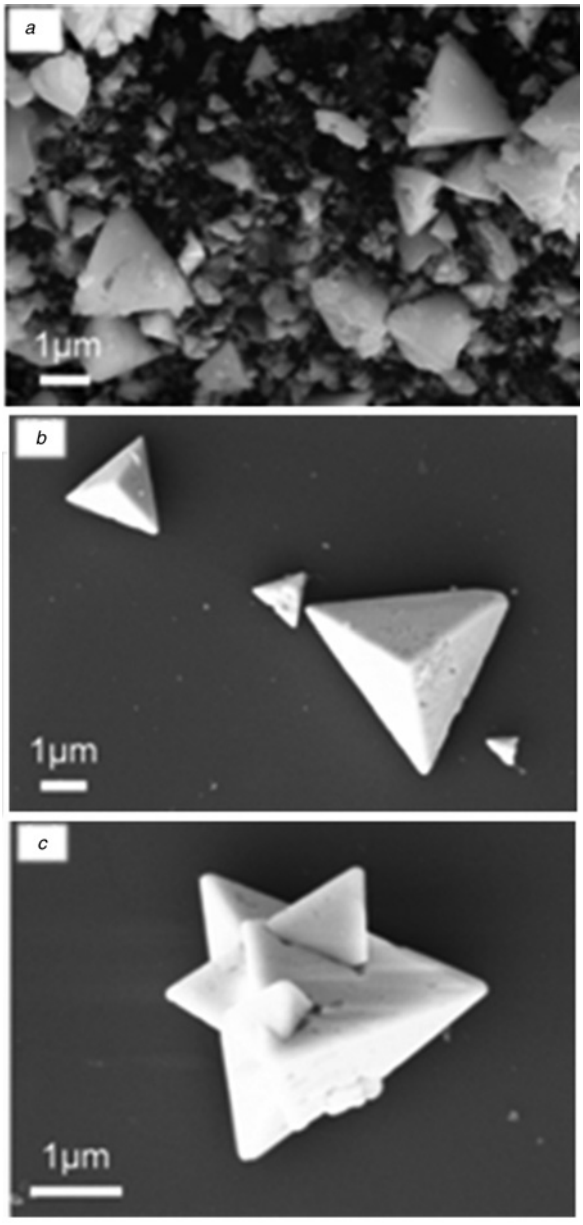

Fig. 3 *SEM images of the tetrahedral γ-Bi_2O_3*
a pH = 8
b pH = 12
c Embeds and stacks on others

doi: 10.1049/mnl.2018.5179

tetrahedron products with the edge length 1–5 μm are observed in images. The surfaces of tetrahedron are quite smooth and every facet is regular triangle. Moreover, a novel phenomenon also could be seen that a part of one tetrahedron embeds into another or some stack on others as shown in Fig. 3*c*, which might originate from a cross and stack-based growth. On the basis of experimental observations from Fig. 3, the growth of single tetrahedron should be completed by two steps, i.e. the formation of nanosheets and their subsequent self-assemble process [18].

3.2.2. Platelet: In addition, the influence of reaction time and their ways on the morphology and crystal structure of the final products was also investigated. Fig. 4 displays the XRD pattern and SEM images of the products refluxing at 90°C for 1 h. Then the experiment was interrupted, after 3 h, the reaction continued for 5 h. Although γ-Bi_2O_3 is the dominant phase, a part of peaks of $Bi_2O_{17}(NO_3)_2$ is also observed on XRD pattern as shown in Fig. 4. The hierarchical Bi_2O_3 microcrystals in Fig. 4*a* are composed of multiple thin platelets, which are smaller than 4 μm in size and exhibit tower-like characteristic. There are displacements between the neighbouring thin platelets, which helps form layered steps along a certain direction. In Fig. 3*b*, it is found that each Bi_2O_3 in these agglomerations is still of plate-like morphology, while they grow together and connect with each other closely which are smaller than 15 nm in thickness. When the reaction was discontinuity, since the energy for reaction is insufficient; Bi^{3+} cannot convert to Bi_2O_3 completely, resulting in low yield of Bi_2O_3. It is supposed that keeping reaction continued was contributed to the formation of Bi–O–Bi bridges between the non-bridging structural hydroxyl groups present in the solution [18, 19].

3.3. Infrared absorption spectra: In order to further confirm that the as-prepared products were composed of γ-Bi_2O_3 phase, Fourier transform infrared spectroscopy spectra of the samples have been examined from 400 to 1300 cm^{-1} as shown in Fig. 5. As we known, the stable coordination number of Bi^{3+} ion is three or six. Cheng *et al.* [20] have reported that the existence of the bands around 830 and 465 cm^{-1} in the infrared spectra of Bi_2O_3 powder shows the presence of $[BiO_3]^{3-}$ polyhedron and $[BiO_6]^{9-}$ octahedral units, respectively. In Fig. 5, the appearance of absorption bands at 830 and 465 cm^{-1} indicates the presence of $[BiO_3]^{3-}$ polyhedron and $[BiO_6]^{9-}$ octahedral units in Bi_2O_3 samples, which is completely agreement with the reports of Cheng *et al.* [20]. Therefore, the

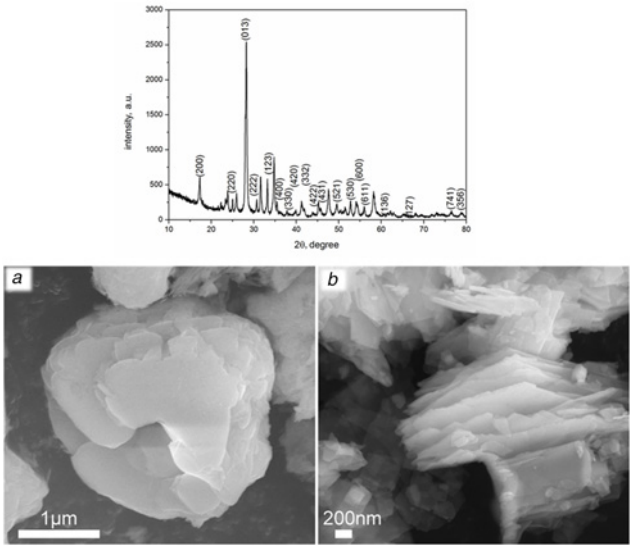

Fig. 4 *XRD pattern of the as-synthesised products and SEM images of the platelet Bi_2O_3*

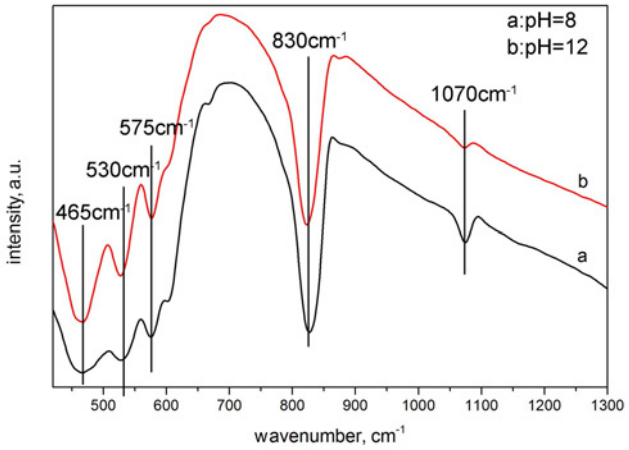

Fig. 5 *IR absorption spectra of as-prepared γ-Bi_2O_3 powder (pH = 8 and pH = 12)*

products are indeed build up by both $[BiO_3]^{3-}$ polyhedron and $[BiO_6]^{9-}$ octahedral units. The peaks at 465 cm^{-1} of two samples are typical Bi^{3+} vibration cause by $[BiO_6]^{9-}$ octahedral units [20]. The bands at 530 and 575 cm^{-1} are also related to the $[BiO_6]^{9-}$ octahedral. While as reported by Pan *et al.*, the strong band centred at 830 cm^{-1} is related to stretching vibration of Bi–O in $[BiO_3]^{3-}$ polyhedron units [21]. The band at 1070 cm^{-1} corresponds to the stretching vibrations of N–O bond. With the content of Bi_2O_3 increased, the intensity of the band decreased which implies that $[BiO_3]^{3-}$ vibration decreases with the content of Bi_2O_3 increasing.

3.4. Optical absorption spectra: The optical properties of Bi_2O_3 powders with pH value of 8 and 12 were characterised by UV–Vis. Fig. 2*a* presents their absorption spectra from 300 to 600 nm in UV–Vis range. The steep absorption edges of both spectra showed their strong absorbance for UV–Vis light. The steep shape of both spectra indicates that the optical absorption is caused by the band gap transition [22]. The band gap of as-synthesised Bi_2O_3 crystals was calculated following Tauc's equation [23]:

$$\alpha h\nu = A(h\nu - Eg)^n$$

where α is the absorption coefficient, h is Planck's constant, ν is the light frequency, E_g is the band gap, A is a constant, and the value of n for direct or indirect allowed transitions can be either 1/2 or 2, respectively. When using $n = 2$, the plot did not show a steep absorption edge, which indicates that indirect transitions are not allowed on this occasion. However, as presented in Fig. 2*b*, the plot of $(\alpha h\nu)^2$ versus $(h\nu)$ showed good straight lines, which is well consistent with the direct transition and the results indicate $n = 1/2$. The band gap of Bi_2O_3 samples can be estimated by the intercept of the tangent in the plot. The band gap was both of 3.0 eV for the Bi_2O_3 crystals prepared in different pH value, which corresponds to 439 nm band-edge in the visible light range.

4. Conclusion: Bi_2O_3 microcrystals with two different morphologies were fabricated by the low-temperature liquid phase method using $Bi(NO_3)_3{\cdot}5H_2O$ and NaOH as raw materials. Bi_2O_3 microcrystals were obtained at a relatively low temperature of 90°C. In our paper, a promising route was presented, which uses no any catalyst, seed or surfactant, and has potential application in large-scale and low-cost production with high quality and might be extended to synthesise other metal oxides. Tetrahedral Bi_2O_3 crystals with the edge length of 1–5 μm and platelet Bi_2O_3 crystals were formed at 90°C for 6 h through different heating

methods. Fourier transform infrared spectra showed that there are two kinds of Bi^{3+} bonds in Bi_2O_3 samples. Finally, the Bi_2O_3 crystals with tetrahedral and platelet morphologies exhibited, their band gap are about 3.0 eV. Consequently, a simple and facile route to synthesise Bi_2O_3 with different morphologies is developed.

5. Acknowledgments: This work was financially supported by National Natural Science Foundation of China (grant no. 11764040), the Key Scientific Research Projects of Colleges and Universities of Xinjiang Uygur Autonomous Region (grant no. XJEDU2016I018) and Natural Science Foundation of Xinjiang Uygur Autonomous Region (grant no. 2017D01C022).

6 References

[1] Yu Y., Lu S., Bao S., *ET AL.*: 'Nanostring-cluster hierarchical structured Bi_2O_3: synthesis, evolution and application in biosensing', *Phys. Chem. Chem. Phys.*, 2016, **18**, (3), pp. 1931–1936

[2] Cabot A., Marsal A., Arbiol L., *ET AL.*: 'Bi_2o_3 as a selective sensing material for NO detection', *Sens. Actu. B*, 2004, **99**, pp. 74–89

[3] Hwang G.H., Han W.K., Park J.S., *ET AL.*: 'An electrochemical sensor based on the reduction of screen-printed bismuth oxide for the determination of trace lead and cadmium', *Sens. Actu. B*, 2008, **135**, pp. 309–316

[4] Gou X., Li R., Wang G., *ET AL.*: 'Room-temperature solution synthesis of Bi_2O_3 nanowire for gas sensing application', *Nanotechnology*, 2009, **20**, pp. 495–501

[5] Xiao X., Hu R, Tu S., *ET AL.*: 'One-pot synthesis of micro/nano structured β-Bi_2O_3 with tunable morphology for highly efficient photocatalytic degradation of methylparaben under visible-light irradiation', *RSC Adv.*, 2015, **5**, (48), pp. 38373–38381

[6] Chen R., Shen Z.R., Wang H., *ET AL.*: 'Fabrication of mesh-like bismuth oxide single crystalline nano flakes and their visible light photocatalytic activity', *J. Alloy Compd.*, 2011, **509**, pp. 2588–2596

[7] Huang Q., Zhang S., Cai C., *ET AL.*: 'β- and α-Bi_2O_3 nanoparticles synthesized via microwave-assisted method and their photocatalytic activity towards the of rhodamine B', *Mater. Lett.*, 2011, **65**, pp. 988–990

[8] Petkov N., Xu J., Morris M.A., *ET AL.*: 'Confined growth and crystallography of one-dimensional Bi_2S_3, CdS, and SnS_x nanostructures within channeled substrates', *J. Phys. Chem. C*, 2008, **112**, pp. 7345–7355

[9] Leontie L., Caraman M., Alexe M., *ET AL.*: 'Structural and optical characteristics of bismuth oxide thin films', *Surf. Sci.*, 2002, **507–510**, pp. 480–485

[10] Gobrecht H., Seeck S., Bergt H.E., *ET AL.*: 'Überuntersuchungen an sismutoxid-aufdampfschichten I. Herstellung sowieelektrsche und optische eigenschaften', *Phys. Stat. Sol. B.*, 1969, **33**, pp. 599–606

[11] Irmawati R., Noorfarizan M.N., Tau fi q-Yap Y.H., Abdul Hamid S.B.: 'Characterization of bismuth oxide catalysts prepared from bismuth trinitrate pentahydrate: in fluence of bismuth concentration', *Cataly Today*, 2004, **93–95**, pp. 701–709

[12] Cheng H.F., Huang B.B., Lu J.B., *ET AL.*: 'Synergistic effect of crystal and electric structure on the visible-light-driven photocatalytic performances of Bi_2O_3 polymorphs', *Phys. Chem. Chem. Phys.*., 2010, **12**, pp. 15468–15475

[13] Liu G., Li S., Lu Y., *ET AL.*: 'Controllable synthesis of α-Bi_2O_3 and ɣ-Bi_2O_3 with high photocatalytic activity byα-Bi_2O_3-ɣ-Bi_2O_3-α-Bi_2O_3 transformation in a facile precipitation method', *J. Alloys Compd*, 2016, **689**, pp. 787–799

[14] Wang Y., Zhao J., Wang Z.: 'A simple low-temperature fabrication of oblique prism-like bismuth oxide via a one-step aqueous process', *Colloid Surf. A*, 2011, **377**, pp. 409–413

[15] Tseng T.K., Choi J., Jung D.W., *ET AL.*: 'Three-dimensional self-assembled hierarchical architectures of gamma-phase flowerlike bismuth oxide', *ACS Appl. Mater. Interf.*, 2010, **2**, pp. 943–946

[16] Wang Y., Li Y.: 'Metastable ɣ-Bi_2O_3 tetrahedra: phase-transition dominated by polyethylene glycol, photoluminescence and implications for internal structure by etch', *J. Colloid Interface Sci.*, 2015, **454**, pp. 238–244

[17] Wu Y.C., Chaing Y.C., Huang C.Y., *ET AL.*: 'Morphology-controllable Bi_2O_3 crystals through an aqueous precipitation method and their photocatalytic performance', *Dyes and Pigments*, 2013, **98**, pp. 25–30

[18] Li W.: 'Facile synthesis of monodisperse Bi_2O_3 nanoparticles', *Mater. Chem. Phys.*, 2006, **99**, pp. 174–180

[19] Yang Q.B., Li Y.X., Yin Q.R., *ET AL.*: 'Hydrothermal synthesis of bismuth oxide needles', *Mater. Lett.*, 2002, **55**, pp. 46–49

[20] Cheng Y., Xiao H.N., Guo W.M.: 'Structure and crystallization kinetics of Bi_2O_3-B_2O_3 glasses', *Thermochim. Acta*, 2006, **444**, pp. 173–178

[21] Pan Z., Henderson D.O., Morgan S.H.: 'Vibrational spectra of bismuth silicate glasses and hydrogen-induced reduction effects', *J. Non-Cryst. Solids*, 1994, **171**, (2), pp. 134–140

[22] Kudo A., Tsuji I., Kato H.: 'Aginzn$_{7}$S$_{9}$ solid solution photocatalyst for H_2 evolution from aqueous solutions under visible light irradiation', *Chem. Comm.*, 2002, **17**, pp. 1958–1959

[23] Tuac T., Grigorovici R., Vancu A.: 'Optical properties and electronic structure of amorphous germanium', *Phys. Status Sol. B*, 1966, **15**, pp. 627–637

doi: 10.1049/mnl.2018.5179